Journal of Geomatics Vol 10 No. 2 October 2016

Vicarious calibration of Resourcesat-2 LISS-III and Landsat 8 OLI sensor data

G.D. Bairagi[1], Sandhya Raikwar[1], V.N. Sridhar[2], Shweta Sharma[2], R.P. Prajapati[2], A.K. Shukla[2], P.K. Verma[1], R. Sharma[1] and Aloke Mathur[2]
[1]M. P. Council of Science and Technology, VigyanBhawan, Bhopal- 462003 (M. P.).
[2]Space Applications Centre, ISRO, DOS, Ahmedabad - 380015
Email: bairagigd@gmail.com

(Received: May 21, 2016; in final form: Oct 03, 2016)

Abstract: The utility of remote sensing is ever increasing, which needs absolute calibration of sensors.It is essential to frequently monitor sensor performance to provide quality data. This study describes a procedure of post-launch calibration for Resourcesat – 2 (RS-2) LISS-III and Landsat 8 OLI bands over crop/ soil at Om Valley, Bhopal, M. P. India. The site is very uniform with radiometric variability of the order of 5% or better, very useful for performing vicarious radiometric calibration to account for characterization of errors or undetermined post-launch changes in spectral response of the sensor. The resultsbased on the study showcalibration coefficient in between 0.95 to 1.05 for RS-2 LIIS-III and Landsat 8 OLI bands.The coefficient values were found consistent on 24April, 18 May and 22 March 2014 satellite passes which indicate that the good calibration stability is exists in RS-2 LISS III and Landsat 8 OLI sensors. The relative errors were found less than 5%, indicating stability of the site. The results demonstrate that the site at Om Valley Bhopal is very useful for performing vicarious radiometric calibration of medium and coarse resolution spacecraft sensors.

Keywords: Spatial, Calibration, Atmosphere, Radiometry, Measurements, Vicarious

1. Introduction

Post- launch calibration is important to remote sensing because it enables a comparison of responses of pre-launch satellite sensors and the ability to monitor their changes over time, which improves the quality of satellite sensor and data products. Calibration and validation are essential activities to ascertain the performance of the satellite sensors and data products. Vicarious calibration provides a method of absolute calibration of sensors using reference and accurate measurements of spectral reflectance using ground instruments. This absolute calibration produces the calibration coefficients that can replace pre-launch laboratory derived coefficients. Prior to launch, on-board calibration (Bruegge et al., 1993) and radiometric calibration (Bruegge et al., 1998) are the parts of calibration procedures.But after the launch, the on-board calibration facility for absolute calibration does not exist. In such cases, a post-launch calibration is needed to compensate for degradation of the satellite sensor (Rao, 2001). Vicarious calibration is a practice to monitor radiometric performance of sensor, which involves the computation of uncertainties in the calibration coefficients to correct the radiometric response of the sensor (Thome et al., 1998).

India's Resourcesat-2 (RS-2) satellite was launched by Polar Satellite Launch Vehicle (PSLV-C16) on 20April, 2011 with LISS - 4 multispectral swath from 23 km to 70 km and improved Radiometric accuracy from 7 bits to 10 bits for LISS - 3 and LISS - 4 and 10 bits to 12 bits for AWiFS sensors. The Landsat 8 Operational Land Imager (OLI) was launched in February 2013. The satellite collects images of the Earth with a 16-day repeat cycle. Vicarious calibration was performed to monitor these in-orbit satellite sensors. This study details the post-launch vicarious calibration performed using high reflectance target site with uniform and flat terrain (OM valley, Bhopal) for visible, Near Infrared (NIR) and Shortwave Infrared (SWIR) bands of the above satellite sensors, for quantifying post-launch changes in the sensor response. The reflectance-based approach was used with field measured surface reflectance and measurements of atmospheric parameters viz. aerosol optical depth (AOD), total columnar ozone and water vapour for the different days of passes. These measured quantities along with spectral response function (pre-launch laboratory measured) were input to the 6S (Second Simulation of a Satellite Signal in the Solar Spectrum) radiative transfer (RT) code (Vermote et al., 2006) for the simulation of top of the atmosphere(TOA) radiance for all the channels. The 6S simulated radiance was compared with the satellite derived radiance to compute the calibration coefficients for all the channels.

2. Study site and satellite data

2.1 Site and its selection

A study site in Bhopal (Om Valley region) was selected to perform vicarious calibration. This site was identified by visual inspection of historical RS-2 LISS-III satellite images followed by field visits and ground verification as per the CEOS guidelines and recommendations for land site selection for vicarious calibration of satellite sensors (Berthelot and Santer, 2008). The site should be spatially and temporally homogeneous with a coefficient of variation ~ 5% or less. This is just a thumb rule since it is difficult to quantify the notion of "homogeneity". Statistically, one measure of homogeneity is the coefficient of variation, which should be as small as possible. The topography of the site presents a smooth and homogenous surface characterized by a good spatial uniformity, which is required for radiometric calibration of sensors. The site was also used for the validation of leaf area index (LAI) product of MODIS (Pandya et al., 2006). A systematic sampling grid of 1×1 km^2 is used for characterizing surface reflectance and for conducting concurrent atmospheric measurements. This choice is dictated partly by practical considerations, viz., the measurements have to be completed preferably within ±1 hour of satellite pass. The satellites under consideration are Landsat-8 and RS 2. The sampling grid of size 60m x60m is used for field measurements of Landsat-8 OLP (30m), RS2-LISS III (24m) and, with appropriate marking of the grid points on the relevant image. The geographic co-ordinates of study site is around 23° 07′ 29.56° N and 77° 25′ 26.08° E.

2.2 Satellites and sensors

The observations were recorded for RS-2 LISS-III and Landsat 8 OLI sensors. The RS-2 LISS-III and Landsat 8 OLI sensor data used in calibration coefficient analysis are 24 April, 18 May and 22 March 2014 respectively. Salient characteristics os sensors are given in Table 1. The Spectro-radiometer, Ozonometer and Sun photometer observation were taken at the time of satellite passes.

3. Methodology

In this study, vicarious calibration was performed using reflectance/ radiance based approach, which was provided by Slater et al. (1987). This technique has been successfully used for satellite's sensor calibration (Biggar et al., 1991, Gellman et al., 1993). In this technique, the RS-2 LISS-III and Landsat 8 OLI derived radiance is compared with 6S simulated TOA radiance. The vicarious radiometric calibration depends on measuring the surface reflectance, path from the sun to earth's surface and earth's surface to sensor and atmospheric optical thickness over a calibration site at the time of satellite overpass. These measurements are used as an input for RT code to simulate an absolute radiance at the sensor level. The field measurements are used to define the spectral directional reflectance of the surface and the spectral optical depth that are used to describe the aerosol and molecular scattering effect in the atmosphere (Gellman et al., 1991) and columnar water vapor to include the water vapor absorption effect. The detailed values of atmospheric parameters are given in table 2.

Table 1: Specifications of the satellite sensors

Bands	Central wavelength (nm)*	Nominal bandwidth (nm)	Lmax ($mw/cm^2/sr/\mu m$)	Lmin ($mw/cm^2/sr/\mu m$)
Resourcesat-2 LISS-III (24 April & 18 May 2014)				
B2-Green	558	520 – 590	52.00	0
B3-Red	654	620 – 680	47.00	0
B4-NIR	821	770 – 860	31.50	0
B5-SWIR	1629	1550 – 1700	7.50	0
Landsat-8 OLI (22 March 2014)			**Grescale***	**Brescale****
B2-Blue (30m)	509	450-510	0.012952	-64.75853
B3-Green (30m)	550	530-590	0.011935	-59.67443
B4-Red (30m)	656	640-670	0.010064	-50.32084
B5-NIR (30m)	859	850-880	0.0061588	-30.79385
B6-SWIR1 (30m)	1633	1570 - 1650	0.0015316	-07.65815
B7-SWIR2 (30m)	2255	2110 - 2290	0.00051624	-02.58121
B8-Pan (15m)	663	500-680	0.011390	-56.94935

*Defined as wavelength at peak response (unity) of spectral response function.

** These are used to convert quantized DN image values to radiance.

Journal of Geomatics Vol 10 No. 2 October 2016

Table 2: Solar angles and atmospheric input parameters for 6S Radiative Transfer code

Date	Sun zenith (deg)	Sun azimuth (deg)	AOT at 550 nm	Water Vapour (g/cm^2)	Ozone (cm-atm)
18.01.2014	47.6951	154.7900	0.4701	1.1360	0.3001
30.01.2014	45.4025	152.2090	0.1802	1.1360	0.3108
02.02.2014	47.6192	144.6800	0.2400	1.1360	0.3100
11.02.2014	42.2931	149.4623	0.2003	1.5800	0.2840
18.02.2014	43.4288	140.4186	0.1501	1.5800	0.2845
19.03.2014	29.2026	141.8605	0.3110	0.7620	0.3046
22.03.2014	32.9876	129.5699	0.2221	0.7620	0.3000
31.03.2014	25.8455	134.5823	0.3923	1.5420	0.2826
12.04.2014	20.9343	131.1497	0.4210	1.2020	0.3423
23.04.2014	25.2928	110.6530	0.3921	1.9930	0.3000
24.04.2014	13.4407	138.2990	0.4223	1.2020	0.3423
18.05.2014	16.8460	098.9616	0.6312	2.9360	0.3000
30.05.2014	13.8820	092.7491	0.5411	2.5860	0.3000

The 6S RT code was used to compute the radiance using ground measurements, which predicts the satellite signal at TOA level using field measurements. The 6S RT model is a generic physically based model. The model utilizes gaseous absorption and scattering by aerosols and molecules. 6S performs better for atmospheric scattering as compared to other RT models (Markham et al., 1992). 6S model was formulated for the atmospheric correction in all the wavelengths. Figure 1 describes the flow chart to simulate radiance at TOA and vicarious calibration coefficient. The US 62 standard atmosphere profile provides the profiles of water vapor, ozone, pressure and temperature up to 100km, at discrete intervals of 34 layers in the 6S RT model (Vermote et al., 2006). Pre-launch laboratory measurements of spectral response function (SRF) were used as an input. Both the SRF and ground reflectance data are resampled to 2.5 nm intervals using spline interpolation method.

The 6S computes TOA radiance and atmospherically corrected surface reflectance in the forward and inverse mode respectively. 6S RT model provides an output in the form of TOA radiance, which is divided by the corresponding radiance observed by the satellite sensors to yield vicarious calibration coefficients. Same as this, 6S provides atmospherically corrected reflectance as an output for a given radiance in the inverse mode, which are compared with the ground measured reflectance by Spectroradiometer.

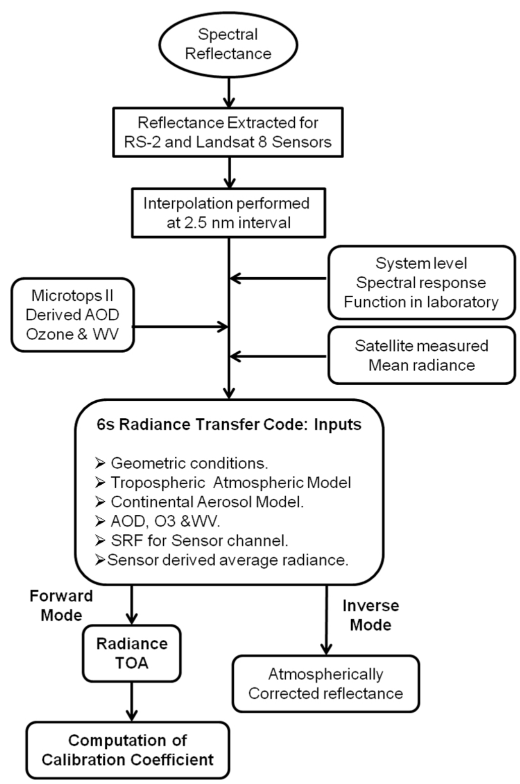

Figure 1: Flow chart for the simulation of TOA radiance and calibration coefficient

4. Results and discussions

This section brings out the recent in-situ measurements and results of experiments conducted over Om Valley, Bhopal site. This exercise was conceived during developmental phase and as part of operationalization of the site. Efforts have been made to process the data to demonstrate the capability and working of the site. The RS-2 LISS III and Landsat 8 OLI cloud free data were used in the analysis.

4.1 Atmospheric measurements

The measured values of AOD, water vapour (g/cm^2) and ozone content using Microtops II are given in Figures 2 and 3 respectively. Variation of AOD with wavelength λ (in nm) was fitted by the Angstrom power law: AOD (λ) = βλ−α for all dates. The Angstrom coefficients α and β were computed by fitting the Angstrom power law at five wavelengths, viz, 0.38, 0.50, 0.675, 0.87 and 1.02 µm. The AOT at 550 nm, required as an input to the 6S atmospheric correction code, was then estimated using α and β coefficients. Both coefficients and average value of AOD at 550 nm are given in figure 2. As expected, the spatial variability of the measured AOT was found to be noticeable with a coefficient of variation ranging between 2-8% for all dates. This means that there is little variability in aerosol within the measurement period of ± 1 hour, over the sampling sites. However, as seen in Figure 2, the temporal variation of AOT across dates is quite high for AOT at all wavelengths. From Figure 2, it is seen that the estimated AOT at 550 nm is high on 18 May (0.63). According to the 6S code manual, any AOT value > 0.65 should not be used for atmospheric correction. Such dates are not considered for vicarious gain computation. It is seen from Figure 3 that ozone is quite stable across all dates while precipitable water content (PWC) shows high variability.

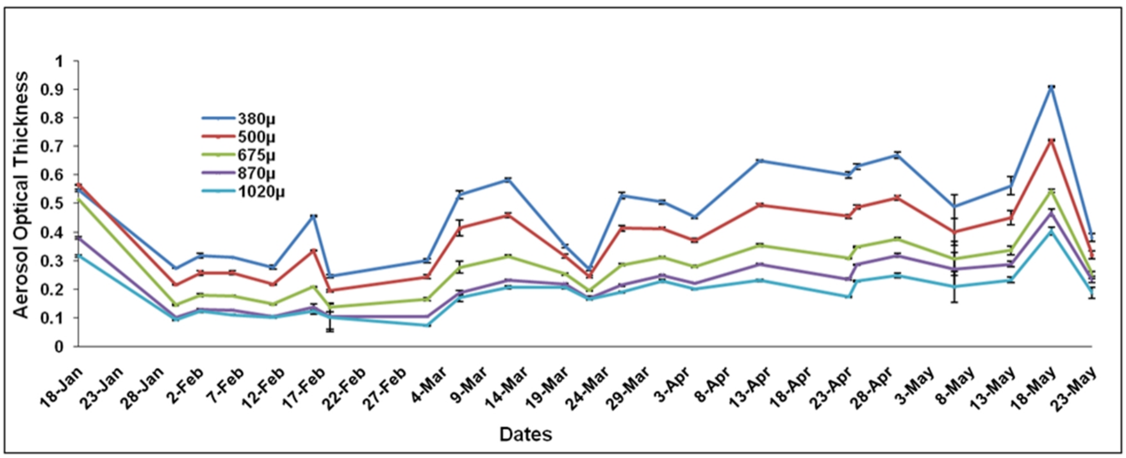

Figure 2: Variation of aerosol optical depth at different wavelengths during 2014

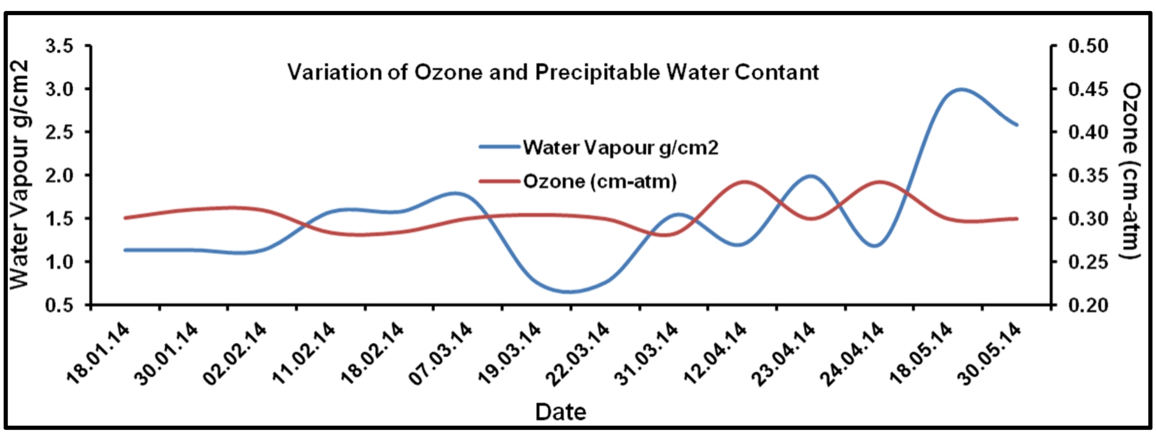

Figure 3: Variation of Ozone (cm-atm) and precipitable water content (gm/cm^2)

4.2 Resourcesat 2 LISS III calibration

The 6S simulated TOA radiance was compared with the RS-2 LISS III radiance. The result of combined linear regression for Green, Red, NIR and SWIR bands are shown in figure 4. The good statistical agreement was observed between satellite-derived radiance and simulated radiance, with R^2 values of 0.999 and 0.993 for the RS-2 LISS III bands for 24April and 18 May 2014, respectively. The bias between satellite-derived radiance and 6S simulated radiance is small, with the values of 1.01 $Wm^{-2}sr^{-1}\mu m^{-1}$ and 1.02 $Wm^{-2}sr^{-1}\mu m^{-1}$ for 24 April and 18 May 2014, respectively.

The details of the Relative Errors (RE) between the 6S simulated and satellite derived radiance is presented in Table 3. It is observed form the Table 3 that the RE values ranges from ±1.5% to 5.0% in all the channels. Similarly, atmospherically corrected surface reflectance was estimated using 6S code in inverse mode. The 6S simulated atmospherically corrected surface reflectance was compared with the field reflectance for RS-2 LISS III channels (Table 4). The field reflectance from spectral radiometer for RS-2 LISS III channels are compared with the 6S simulated atmospherically corrected reflectance shows RE values from ±2.1% to 4.7% in all the channels.

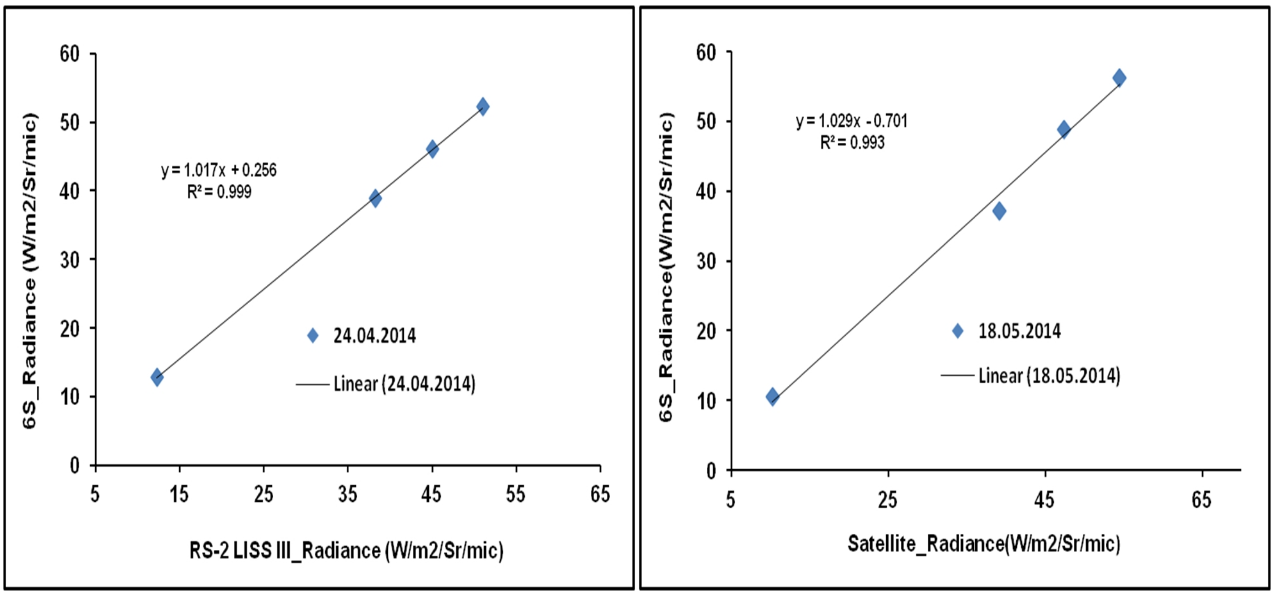

Figure 4: Comparison of 6S radiance with RS-2 LISS III radiance of different bands for 24 April and 18 May 2014

Table 3:Values of radiance and calibration coefficient for 24 April and 18 May 2014 satellite passes

Channels	RS-2 LISS-III Radiance (w/m2/sr/m)	6S Simulated Radiance (w/m^2/sr/m)	Relative Errors In Radiance(%)	Calibration Coefficient
24 April 2014				
Green	50.916	52.266	2.6	0.974
Red	45.024	46.050	2.2	0.978
NIR	38.233	38.836	1.5	0.984
SWIR	12.247	12.819	4.6	0.955
18 May 2014				
Green	54.474	56.289	3.3	0.968
Red	47.436	48.912	3.1	0.970
NIR	39.131	37.145	-5.0	1.053
SWIR	10.199	10.512	3.0	0.970

Table 4: The values of reflectance summarized for both the passes of the RS-2 LISS III sensor

Channels	Ground Measured Reflectance	6S simulated atmospherically corrected Reflectance	Relative Errors in Reflectance (%)
24.04.2014			
Green	0.05990	0.06218	3.8
Red	0.07908	0.08240	4.2
NIR	0.11550	0.11882	2.8
SWIR	0.18647	0.19044	2.1
18.05.2014			
Green	0.05826	0.060397	3.6
Red	0.07211	0.075545	4.7
NIR	0.11675	0.112676	-3.4
SWIR	0.15267	0.159318	4.3

4.3 Landsat 8 OLI calibration

The 6S simulated TOA radiance was compared with the Landsat 8 OLI radiance. The result of combined linear regression for all seven bands is shown in figure 5. The good statistical agreement was observed between satellite-derived radiance and simulated radiance, with R^2 values of 0.99 for the Landsat 8 OLI channels on 22 March 2014. The bias between satellite-derived radiance and 6S simulated radiance is small, with the values of 0.9 $Wm^{-2}sr^{-1}\mu m^{-1}$. The values of the RE between the 6S simulated and satellite derived radiance are presented in Table 5. It is observed form the Table 5 that in case of Landsat 8 OLI channels RE estimates of the radiance values are ranging from ±0.6% to 5.4% in all the channels. The 6S simulated atmospherically corrected surface reflectance was compared with the field reflectance using radiometer for Landsat 8 OLI channels (Table 6). The field reflectance from Spectroradiometer for Landsat 8 OLI channels are compared with the 6S simulated atmospherically corrected reflectance shows relative error estimates from ±0.9% to 7.8% in all the channels.

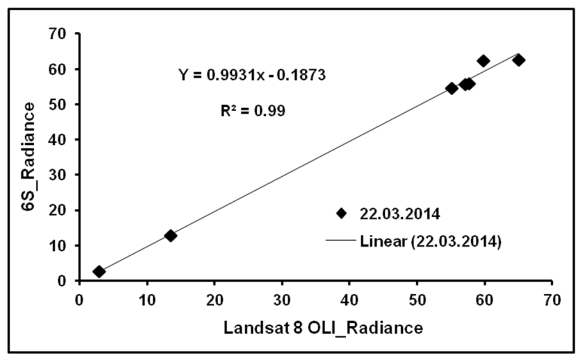

Figure 5: Comparison of 6S radiance with Landsat 8 OLI radiance for all the bands

Table 5: The values of radiance and calibration coefficient are summarized for the Landsat 8 OLI sensor

Channels	Landsat-8 Radiance ($w/m^2/sr/m$)	6S Simulated Radiance ($w/m^2/sr/m$)	Relative Errors in Radiance (%)	Calibration Coefficient
Blue	65.0119	62.6250	-3.6	1.03
Green	57.5919	56.0190	-2.7	1.02
Red	55.0878	54.7390	-0.6	1.00
NIR	59.7046	62.5150	4.7	0.95
SWIR1	13.4391	12.9620	-3.5	1.03
SWIR2	02.8939	02.7370	-5.4	1.05
Pan	57.0664	55.7340	-2.3	1.02

Table 6: The values of reflectance summarized for the Landsat 8 OLI sensor

Channels	Ground Measured Reflectance	6S simulated atmospherically corrected Reflectance	Relative Errors in Reflectance (%)	Calibration Coefficient
Blue	0.0519	0.0530	2.7	0.98
Green	0.0872	0.0920	5.1	0.95
Red	0.1207	0.1220	0.9	0.99
NIR	0.2430	0.2320	-4.5	1.05
SWIR1	0.2067	0.2150	3.8	0.96
SWIR2	0.1330	0.1400	7.6	0.95
Pan	0.0966	0.1010	4.6	0.96

4.4 Vicarious calibration coefficient

Figure 6 and tables 3 and 4 describe the mean TOA radiance, surface reflectance and vicarious calibration coefficient derived from measurements at the Om Valley site for two dates. From figure 6, the mean values of simulated and satellite observed radiance are in agreement for all the channels of RS-2 LISS III sensor. The differences between simulated and observed radiance are very small which may be due to the intrinsic variability and meteorological variability of the site.

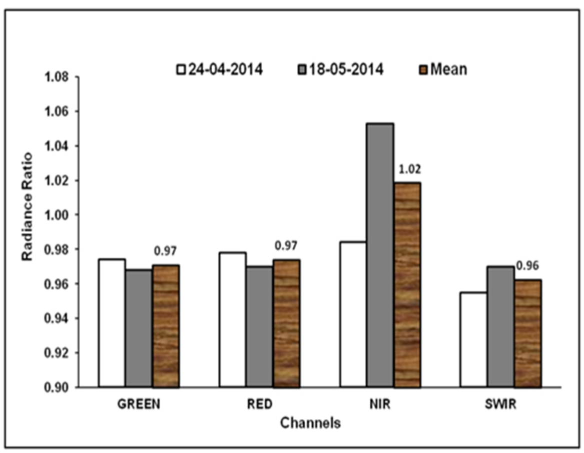

Figure 6: Variation of 6s radiance and RS-2 LISS III radiance and mean value of vicarious bands

The vicarious calibration coefficient is the ratio of 6S simulated radiance and satellite observed radiance. For an ideal case, if there is no degradation in the sensor after launch and ground and atmosphere are absolutely characterized and have an accurate RT code, simulated TOA radiance should precisely match with satellite observed radiance. It means the ratio of simulated to observed radiance should be unity. In practice it is not possible, there are uncertainties in field reflectance and atmospheric measurements, modelling uncertainties in the RT code. Figure 6 describes the ratio of the TOA radiance simulated using ground measured data to the RS-2 LISS III sensor derived radiance for the channel and day along with average value. The vicarious calibration coefficient data for RS-2 LISS III sensor indicate minor changes in the calibration of RS-2 LISS III sensor for all the channels and the changes are ranging in between ±0.04 (figure 6). The SE of the calibration coefficient is less than 5% for the all the channels. Patel et al. (2014) also found that the INSAT-3D imager overestimates TOA radiance in the visible band by5.1% and in the SWIR band by 11.7% with respect to 6S simulated radiance. For these bands, in the inverse mode, the 6S corrected surface reflectance was closer to field surface reflectance.

Table 5 describes the ratio of the TOA radiance simulated using ground measured data to the Landsat 8 OLI sensor derived radiance for all the channels for 22 March 2014. The vicarious calibration coefficient data for Landsat 8 OLI sensor shows variations ±0.05 in the calibration coefficient for all the channels. The relative percentage error at all the channels for different days describes in Tables 3 and 6. The RE are found to be less than 5%. Errors are observed high in Red channel. The errors may be associated with uncertainties in the atmospheric conditions or due to surface variation. The noted values were found to be consistent, which indicate good calibration stability of RS-2 LISS III sensor and Landsat 8 OLI sensor.

5. Summary and conclusion

This study brings out the results of calibration site at Om Valley, Bhopal. In this study, post-launch calibration was performed for the RS-2 LISS-III and Landsat 8 OLI sensors over the homogeneous areaof

Om Valley, Bhopal. The TOA radiance was simulated by 6S RT model using ground measurements taken synchronous to the satellite over passes study site. The conclusions made based on the study are, radiance calibration coefficient is maintained 0.95 to 1.05 forRS-2 LIIS-III and Landsat 8 OLI for all the bands. The coefficient values were found consistent, which indicate that the good calibration stability is of RS-2 LISS III and Landsat 8 OLI sensors. The relative errors were found less than 5%, indicating stability of the site. The results show that the site at Om Valley Bhopal is very uniform with radiometric variability of the order of 5% or better, very useful for performing vicarious absolute radiometric calibration of medium and coarse resolution spacecraft sensors.

References

Berthelot, B and R. Santer (2008). Adequacy of the selected sites with respect to the atmospheric/surface parameters. CALIB-TN-WP230-VEGA_001.pdf.

Bruegge, C.J., V.G. Duval, N.L. Chrien, R.P. Korechoff, B.J. Gaitley and E.B. Hochberg (1998). MISR prelaunch instrument calibration and characterization results. IEEE Transactions on Geoscience and Remote Sensing, 36, pp. 1186–1198.

Bruegge, C.J., A.E. Stiegman, R.A. Rainen and A.W. Springsteen (1993). Use of Spectralon as a diffuse reflectance standard for in-flight calibration of earth-orbiting sensors. Optical Engineering, 32, pp. 805–814.

Gellman, D.I., S.F. Biggar, M.C. Dinguirard, P.J. Henry, M.S. Moran, K.J. Thome and P.N. Slater (1993). Review of SPOT-1 and -2 calibrations at White Sands from Launch to the Present. Proc. SPIE. 1938. pp. 118-125.

Gellman, D.I., S.F. Biggar, P.N. Slater and C.J. Bruegge (1991). Calibrated intercepts for solar radiometers used in remote sensor calibration. Proc. SPIE, 1493, pp. 19–24.

Markham, B.L., R.N. Halthore and S.J. Goetz (1992). Surface reflectance retrieval from satellite and aircraft sensors: Results of sensor and algorithm comparison during FIFE. Journal of Geophysical Research, 97 (D17), pp. 18785-18795.

Pandya, M.R., R.P. Singh, K.N. Chaudhari, G.D. Bairagi, R. Sharma, V.K. Dadhwal and J.S. Parihar (2006). Leaf area index retrieval using IRS LISS-III sensor data and validation of the MODIS LAI product over central India. IEEE Transactions on Geosciences and Remote Sensing, 44(7):1858 – 1865.

Patel, Piyush Kumar, Hiren Bhatt and A.K. Shukla (2014). Absolute vicarious calibration of recently launched Indian meteorological satellite: INSAT – 3D imager. International Archives of the Photogrammetry, Remote Sensing and Spatial Information Sciences, Volume XL-8, 2014, ISPRS Technical Commission VIII Symposium, 09 – 12 December 2014, Hyderabad, India, Pp, 291-298.

Rao, C.R.N. (2001). Implementation of the Post-launch vicarious calibration of the GOES imager visible channel. (Camp Springs, MD: NOAA Satellite and Information Services (NOAA/NESDIS)), http://www.ospo.noaa.gov/Operations/GOES/calibration/vicar ious-calibration.html.

Slater, P.N., S.F. Biggar, R.G. Holm, R.D. Jackson, Y. Mao, M.S. Moran, J.M. Palmer and B. Yuan (1987). Reflectance and radiance-based methods for the in-flight absolute calibration of multispectral sensors. Remote Sensing of Environment. 22. pp. 11–37.

Thome,K., K.S. Schiller, J. Conel, K. Araiand S. Tsuchida (1998). Results of the 1997 Earth observing system vicarious calibration joint campaign at Lunar Lake Playa, Nevada (USA). Metrologia. 35. pp. 631–638.

Vermote, E., D. Tanre, J.L. Deuze, M. Herman, J.J. Morcrette and S.Y. Kotchenova (2006). Second Simulation of Satellite Signal in the Satellite Spectrum (6S). 6S User Guide Version 3. University of Maryland.